proceedings

MDPI

Proceedings

Mechanical Characterization of Compact Basalt by Using SHPB Device †

Sunita Mishra *, Tanusree Chakraborty and Vasant Matsagar

Department of Civil Engineering, Indian Institute of Technology (IIT) Delhi, Hauz Khas, New Delhi 110 016, India; tanusree@civil.iitd.ac.in (T.C.); matsagar@civil.iitd.ac.in (V.M.)

* Correspondence: sunita.mishra256@gmail.com; Tel.: +91-971-725-3877

† Presented at the 18th International Conference on Experimental Mechanics, Brussels, Belgium, 1–5 July 2018.

Published: 9 May 2018

Abstract: In the present work, dynamic stress-strain response of compact basalt is tested under high loading rates using 38 mm split Hopkinson pressure bar (SHPB) device. The physical and static mechanical properties of compact basalt, e.g., density, specific gravity, static compressive strength and elastic modulus values are also determined. Petrological studies of compact basalt are carried out through X-ray diffraction (XRD) test and scanning electron microscope (SEM) test. In the SHPB tests, it is observed from the stress-strain response that the dynamic peak stress increases with increasing strain rate however the elastic modulus is nearly constant with increase in strain rate. Dynamic force equilibrium at the incident and transmission bar ends of the rock samples is attained in all tests till the failure of the rock samples. Dynamic increase factor (*DIF*) for the rock is determined at a particular strain rate by comparing the dynamic to static peak compressive stress. Correlation equation for dynamic strength increase factor with respect to strain rate has been proposed herein.

Keywords: compact basalt; dynamic increase factor; SHPB

1. Introduction

The Deccan trap region formed due to the lava flow in the Mesozoic era covers nearly 20% land area of India. Many major underground tunneling projects are currently underway in this region for southern Indian railways where drilling and blasting activities take place on a regular basis. The region also houses major hydropower projects and underground mining industries. Any natural or manmade hazard in this region may prove to be disastrous causing significant losses to Indian economy and mankind. The loads caused by hazardous events like earthquake and blast are highly transient in nature generating high strain rates in rock. The strain rate caused by blast may reach up to 10^4/s [1,2] which in turn affects both the stiffness and the strength properties of the rocks. Thus, for sustainable design of infrastructure in the Deccan trap region, it becomes necessary to characterize the rocks under static and dynamic loading conditions.

In the recent past, various scientists and researchers have conducted dynamic compression test on rocks and soils by using split Hopkinson pressure bar (SHPB) and dynamic triaxial tests [3–16]. The dynamic strength and fracture properties of Dresser basalt are studied by [5] through uniaxial and triaxial compression tests with radial confining pressure values varying from 0 MPa to 689.47 MPa for strain rates from 10^{-4}/s to 10^3/s and temperatures from 80 K to 1400 K. They observed a strong dependence of the fracture strength of rock on both temperature and rate of deformation. The energy absorptions in two different rocks, i.e. Bohus granite and Solenhofen limestone are studied by [6] and observed that the energy absorbed by the rocks increases markedly when the applied load reaches the critical value of 1.8 and 1.3 times the static compressive strength for Bohus granite and Solenhofen

limestone, respectively. Dynamic triaxial compression test was performed by [7] at strain rates from 10^{-2}/s to 10/s for charcoal granodiorite up to a confining pressure of 0.45 GPa, for Berea sandstone and Indiana limestone up to a confining pressure of 0.25 GPa. They concluded that the differential stress at failure was relatively constant up to a strain rate of 1/s, however, increased when the strain rate was higher than 1/s. [10] conducted dynamic uniaxial compressive test on Bukit Timah granite in Singapore at four different loading rates (10^0 MPa/s, 10^1 MPa/s, 10^3 MPa/s and 10^5 MPa/s). It was concluded from the tests that for each log scale increase in loading rate, the compressive strength of the rock increases by 15% and there were small changes in elastic modulus and Poisson's ratio values. The dynamic stress-strain response of Bukit Timah granite loaded at a medium strain rate of 20/s–60/s using SHPB is reported by [13]. It was observed from the results that the dynamic fracture strength of the granite is directly proportional to the cube root of strain rate whereas the elastic modulus remains unchanged with increasing strain rate. It may be summarized from the literature review that dynamic compressive strength test of rocks using SHPB have been carried out on different rock types, e.g., granite, Barre granite, basalt, volcanic tuff, Kawazu tuff, red sandstone, Indiana limestone, porphyritic tonalite, oil shale, granodiorite, coal, kidney stone, Tennessee marble and Akyoshi marble up to 2000/s strain rate [15] and strain rate has significant effect on the mechanical behavior of rocks but till date, no SHPB tests are performed on rocks from Deccan trap region of the Indian sub-continent.

The objectives of the present work are to characterize an igneous rock from the Deccan trap region i.e. compact basalt under strain rate dependent loading. The compact basalt rock blocks are collected from Koyna Dam, Satara, Maharashtra project site, India. The rock samples have been tested for both physical and mechanical properties.

2. SHPB Test Setup

Figure 1 shows a typical schematic diagram of the compression SHPB test setup. The SHPB in the Rel Inc. laboratory in Calumet, Michigan is designed and manufactured by the Rel Inc. group. The setup comprises of an incident bar, a transmission bar and striker bars of different sizes. The bars are made up of C300 maraging steel with yield strength 300,000 psi (2068.4 MPa). The incident bar length is 2.59 m and diameter is 38.1 mm. The transmission bar length is 2.43 m and diameter is 38.1 mm. The dimensions of the incident and the transmission bars allow one-dimensional loading of the sample. In the present work, four different lengths of striker bars are used, e.g., 139.7 mm, 228.6 mm, 304.8 mm, and 558.6 mm; the diameter of striker bar is 38.1 mm. The striker bar is propelled by a compressed air gas gun at varying pressure magnitudes which generate stress waves inside the striker bar. The striker bar hits the impact end of the incident bar and remains in contact till the stress wave travels from one end of the striker bar to the other end. The compressive stress wave upon reaching the other free end of the striker bar gets reflected back as a tensile wave. As a result, the contact between the striker bar and the incident bar is lost. The time duration taken by the stress wave to travel from one end of the striker bar to the other end is the total loading time of the sample given by

$$\Delta t = 2L_{\mathrm{s}} / c_{\mathrm{bar}} \quad (1)$$

where, L_s is the length of the striker bar and cbar is one-dimensional longitudinal stress wave velocity in the bar. Thus, using longer striker bar increases the loading time and the rock sample gets time to respond. As a result, lower strain rate develops when longer striker bar is used. For smaller striker bars, the time taken by the stress wave to propagate from one end to the other end of the bar is less and hence the loading time duration is also less for the same amount of the load intensity which results in higher strain rate. The strains in the incident and the transmission bars are measured using two strain gauges, one mounted on the incident bar and the other mounted on the transmission bar. In order to read the strain signal, Vishay 2310B signal conditioner and amplifier with ¼ Wheatstone bridge have been used with a Picoscope5242 having sampling rate of 1 in 8 nanoseconds. The basic equations of stress, strain and strain rate generated in the sample upon loading van be found in [17].

In the Rel Inc. SHPB system, SurePulse program is used for automatic loading and firing of the striker bar. The velocity of the striker bar is also recorded automatically using the SurePulse program

and fiber optic speed sensors with a response time of 1 μs. Also, the SurePulse program has been used for data processing, e.g., obtaining stress-strain plots, strain and strain rate time histories, force equilibrium at the interfaces of the incident bar—sample and the transmission bar-sample. From these plots, peak stress, average strain rate, dynamic elastic modulus, strain at peak stress, force equilibrium and effect of pulse shapers are studied.

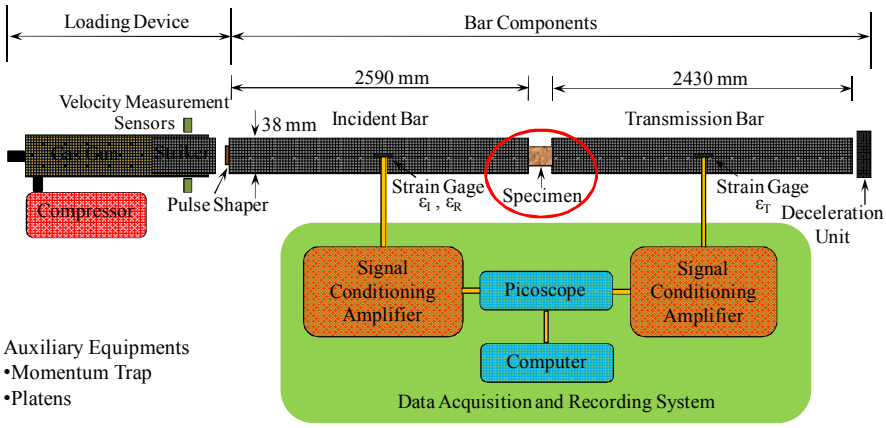

Figure 1. Schematic diagram of 38 mm diameter SHPB device.

3. Results and Discussion

3.1. Physical Properties

The physical properties of the rocks are presented in Table 1. The dry density value of compact basalt is determined for five samples and the average value is taken to be 2927 kg/m^3. The specific gravity values of compact basalt is estimated to be 2.89. The density and specific gravity values of compact basalt is compared with the available data from the literature and observed to be well in agreement [18,19].

Table 1. Physical and static properties.

Rocks	Dry Density, ϱ_d (kg/m^3)	Specific Gravity, G	Uniaxial Compressive Strength, σ_c (MPa)	Modulus of Elasticity, E_t (GPa)
Compact Basalt	2927	2.89	58.58	24.00

3.2. Results of Petrological Studies

Figures 2a,b present the SEM images, and the XRD graphs. It is observed in the SEM images that the grains are crystalline in structure. The quartz grains can be identified from the SEM images as white spots. Now, the mineral content of the rock specimens is confirmed by the XRD graphs. The mineralogy of basalt is ascertained to be calcic plagioclase feldspar with augite of pyroxene group, olivine, amphibole, magnetite, quartz, and hornblende. The XRD graphs of compact basalt is compared with the available data from the literature and observed to be well in agreement [20].

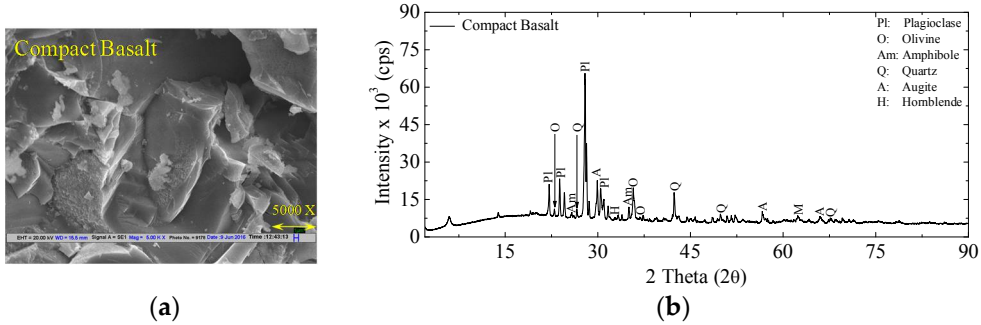

(**a**) (**b**)

Figure 2. (**a**) Scanning electron microscope images and (**b**) X-ray diffraction test graphs of compact basalt.

3.3. Static Uniaxial Compressive Strength

The rock specimens are prepared and tested by following ASTM and ISRM standards [22,23] for evaluating the static uniaxial compressive strength. The rock specimens were tested at 0.001/s strain rate to determine the uniaxial compressive strength. The tests on each type of rock are repeated three times and the average strength values are presented in Table 1. The static uniaxial compressive strength of compact basalt is found to be 58.58 MPa. The elastic modulus from the stress-strain graph at 50% of peak stress value is calculated to be 24.00 GPa [24]. The static uniaxial compressive strength of the tested rock is compared with the available data from the literature and observed to be well in agreement [19,20].

3.4. Stress-Strain Response for Compact Basalt

The dynamic tests are conducted on compact basalt with total 15 number of rock specimens. The specimens prepared with 38 mm diameter and slenderness ratio of 0.5 and tested by following ISRM suggested methods [24]. The incident and transmission waveforms for compact basalt is shown in Figure 3. The post processing of the waveforms is done to obtain the stress-strain response of the rock specimens tested following [17]. The stress-strain response curves for compact basalt are obtained from SHPB tests for different strain rates varying from 41.31/s to 475.59/s and are shown in Figure 3. The pressure is varied from 25 psi to 60 psi with varying striker bar length generating strain rates from 41.31/s to 475.59/s in the rock samples. The dynamic properties of the rock specimens for compact basalt e.g., peak stress, dynamic elastic modulus, the strain at peak stress, and dynamic increase factor at different strain rates generated by varying pressure in the gas gun, velocity of the striker bar, and pulse shaper are presented in Table 2. It is observed from the test results that the peak stress increases by almost 39% from strain rate 41.31/s to 186.7/s and by 31% from strain rate 186.7/s to 457.59/s. The dynamic elastic modulus is calculated at 50% of the peak stress value. It is seen from Table 2 that the dynamic elastic modulus of compact basalt is nearly constant to an average value of 32.57 GPa for the strain rate range tested herein. Moreover, it is observed that the dynamic elastic modulus is similar to the static elastic modulus. Hence, it can be concluded that the peak stress is sensitive to strain rate whereas the elastic modulus is not sensitive to strain rate.

Table 2. Dynamic properties: compact basalt.

S.R.R.	S.N.	l (mm)	d (mm)	L_s (mm)	P_s (psi)	V_{st} (m/s)	$\dot{\varepsilon}$ (/s)	σ_{dc} (MPa)	ε	E_d (GPa)	*DIF*
Low	B7	18.08	37.16	558.8	32	13.16	41.31	242.84	0.011	31.19	4.14
	B6	17.34	37.26	228.6	25	15.72	61.76	255.68	0.007	33.88	4.36
	B8	18.79	37.26		35	16.72	72.68	229.64	0.009	19.79	3.92
Medium	B11	16.71	37.23	228.6	74	33.95	81.71	328.48	0.008	31.77	5.60
	B12	16.12	37.31	304.8	30	17.58	97.86	249.14	0.008	31.94	4.25
	B5	16.51	37.77	139.7	45	25.78	106.22	319.93	0.011	31.94	5.46
	B007	18.67	37.26	304.8	50	22.98	139.44	350.35	0.009	67.43	5.98
	B1	15.36	37.33	139.7	45	30.01	159.44	348.32	0.012	26.65	5.94
High	B3	17.67	37.77	139.7	45	32.06	186.70	337.13	0.011	30.16	5.75
	B17	18.67	37.26	228.6	60	28.31	246.95	393.88	0.012	39.11	6.72
	B16	18.92	37.26	228.6	60	28.11	248.18	414.75	0.012	43.77	7.08
	B15	17.62	37.26		60	28.93	475.59	440.87	0.016	25.32	7.52

* S.R.R. = Strain rate range, S.N. = Sample number, l = Sample length, d = Sample diameter, L_s = Striker nar length, P_s = Striker bar pressure, V_{st} = Striker bar velocity, $\dot{\varepsilon}$ = Strain rate, σ_{dc} = Dynamic peak stress, ε = Strain at peak stress, E_d = Dynamic Elastic modulus, *DIF* =Dynamic Increase Factor.

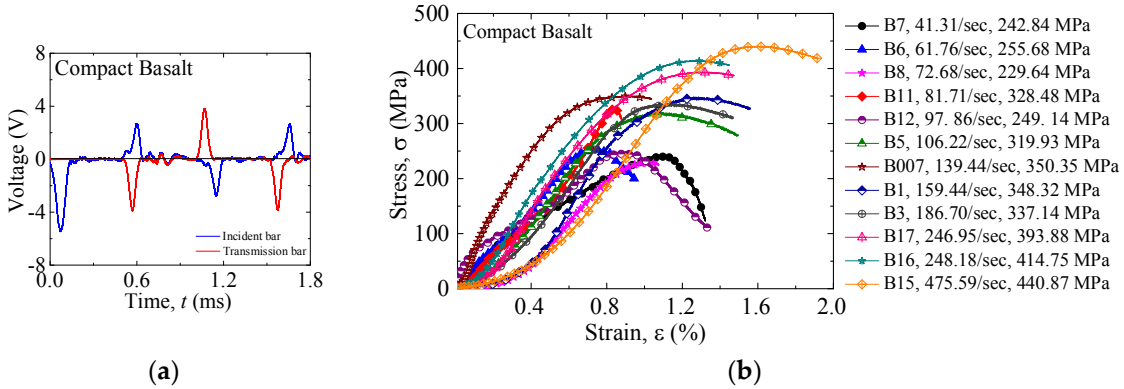

Figure 3. (**a**) Waveform obtained from SHPB tests and (**b**) Stress-strain response of compact basalt.

3.5. Dynamic Increase Factor and Proposed Correlation Equation

The dynamic increase factors (*DIF*) have been determined by comparing the dynamic peak stress with the static peak stress. The *DIF* values of the tested rock specimens are reported in Table 2. The *DIF* values are also plotted in Figure 4 for compact basalt. It may be seen from Table 2 that the dynamic compressive strength of compact basalt is 4.14 to 7.52 times that of the static compressive strength for strain rates varying from 41.31/s to 475.59/s.

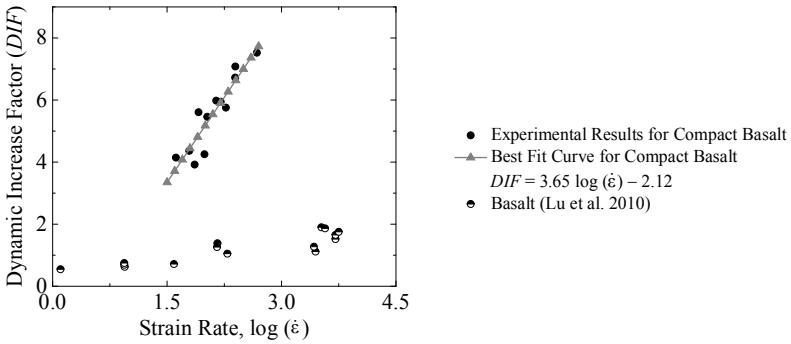

Figure 4. Dynamic increase factor vs strain rate response for compact basalt.

The correlation equation for compact basalt with a coefficient of determination (R^2) = 0.84 is presented in Figure 4 and given by

$$DIF = 3.65\log(\dot{\varepsilon}) - 2.12 \text{ for } 41.31/\text{sec} \le \dot{\varepsilon} \le 457.59/\text{sec} \quad (2)$$

It may be noted that the *DIF* equation proposed herein will be applicable for the strain rate ranges considered in the current work. The *DIF* correlation thus developed for the given strain rate range can be used as a material model in the dynamic analysis of underground structures and in blast-resistant designs.

4. Conclusions

In the present study, the following conclusions are drawn from the high strain rate characterization of an igneous rocks e.g., compact basalt using uniaxial compressive SHPB device. The peak stress increases by almost 39% from strain rate 41.31/s to 186.7/s and by 31% from strain rate 186.7/s to 457.59/s. The dynamic elastic modulus of compact basalt is nearly constant to an average value of 32.57 GPa for the strain rate range tested herein which is similar to the static elastic modulus. The dynamic compressive strength is 4.14 to 7.52 times that of the static compressive strength for strain rates range tested and the correlation equation proposed for compact basalt is given by

$$DIF = 3.65\log(\dot{\varepsilon}) - 2.12 \text{ for } 41.31/\text{sec} \le \dot{\varepsilon} \le 457.59/\text{sec}$$

Author Contributions: S.M. is the student in the Department of Civil Engineering, Indian Institute of Technology Delhi, India, who has work on this paper under the supervision of T.C. and V.M., who are presently working in the Department of Civil Engineering, Indian Institute of Technology Delhi, India.

Conflicts of Interest: The authors declare no conflict of interest.

References

1. Ngo, T.; Mendis, P.; Gupta, A.; Ramsay, J. Blast Loading and Blast Effects on Structures—An Overview. *Electr. J. Struct. Eng.* **2007**, *7*, 76–91.
2. Dusenberry, D.O. *Handbook for Blast Resistant Design of Buildings*, 1st ed.; John Wiley and Sons: Hoboken, NJ, USA, 2010; p. 512.
3. Perkins, R.D.; Green, S.J. Macroscopic Description Low and Medium Strain Rates. *Int. J. Rock Mech. Min. Sci.* **1970**, *7*, 527–535.
4. Christensen, R.J.; Swanson, S.R.; Brown, W.S. Split Hopkinson Bar Tests on Rock under Confining Pressure. *Exp. Mech.* **1972**, *12*, 508–541.
5. Lindholm, U.S.; Yeakley, L.M.; Nagy, A. The Dynamic Strength and Fracture Properties of Dresser Basalt. *Int. J. Rock Mech. Min. Sci. Geomech. Abstr.* **1974**, *11*, 181–191.
6. Lundberg, B. A Split Hopkinson Bar Study of Energy Absorption in Dynamic. *Int. J. Rock Mech. Min. Sci. Geomech. Abstr.* **1976**, *13*, 187–197.
7. Blanton, T.L. Effect of Strain Rates from 10^{-2} to 10 s^{-1} in Triaxial Compression Tests on Three Rocks. *Int. J. Rock Mech. Min. Sci. Geomech. Abstr.* **1981**, *18*, 47–62.
8. Klepaczko, J.R. Behavior of Rock-like Materials at High Strain Rates in Compression. *Int. J. Plast.* **1990**, *6*, 415–432.
9. Olsson, W.A. The Compressive Strength of Tuff as a Function of Strain Rate from 10^{-6} to 10^{3}/s. *Int. J. Rock Mech. Min. Sci. Geomech. Abstr.* **1991**, *28*, 115–118.
10. Zhao, J.; Li, H.B.; Wu, M.B.; Li, T.J. Dynamic Uniaxial Compression Tests on a Granite. *Int. J. Rock Mech. Min. Sci.* **1999**, *36*, 273–277.
11. Frew, D.J.; Forrestal, M.J.; Chen, W. A Split Hopkinson Pressure Bar Technique to Determine Compressive Stress-strain Data for Rock Materials. *Exp. Mech.* **2000**, *41*, 40–46.
12. Fukui, K.; Okubo, S.; Ogawa, A. Some Aspects of Loading-Rate Dependency of Sanjome Andesite Strengths. *Int. J. Rock Mech. Min. Sci.* **2004**, *41*, 1215–1219.
13. Li, X.B.; Lok, T.S.; Zhao, J. Dynamic Characteristics of Granite Subjected to Intermediate Loading Rate. Rock Mech. *Rock Eng.* **2005**, *138*, 21–39.
14. Qi, C.Z.; Wang, M.Y.; Qihu, Q. Strain-Rate Effects on the Strength and Fragmentation Size of Rocks. *Int. J. Imp. Eng.* **2009**, *36*, 1355–1364.
15. Lu, Y.B.; Li, Q.M.; Ma, G.W. Numerical Investigation of the Dynamic Compressive Strength of Rocks based on Split Hopkinson Pressure Bar Tests. *Int. J. Rock Mech. Min. Sci.* **2010**, *47*, 829–838.
16. Chakraborty, T.; Mishra, S.; Loukus, J.; Halonen, B.; Bekkala, B. Characterization of three Himalayan Rocks using a Split Hopkinson Pressure Bar. *Int. J. Rock Mech. Min. Sci.* **2016**, *85*, 112–118.
17. Chen, W.; Song, B. *Split Hopkinson (Kolsky) Bar—Design, Testing and Applications*; Springer: Berlin/Heidelberg, Germany, 2011.
18. Jhanwar, J.C.; Goel, R.K.; Chakraborty, A.K.; Bandopadhyay, C. Development of Tunnel Support Guidelines for Tunneling in Basaltic Rocks—A Case Study. In *Proceedings Geomechanics and Ground Control*; Allied Publishers Pvt. Ltd.: Gandhinagar, India, 2003; pp. 29–35.
19. Brandes, H.G.; Robertson, I.N.; Johnson, G.P. Soil and Rock Properties in a Young Volcanic Deposit on the Island of Hawaii. *J. Geotech. Geoenviron. Eng. ASCE* **2011**, *137*, 597–610.
20. Gupta, A.S.; Rao, K.S. Weathering Effects on the Strength and Deformational Behaviour of Crystalline Rocks under Uniaxial Compression State. *Eng. Geol*. **2000**, *56*, 257–274.
21. ASTM International. *Standard Practices for Preparing Rock Core as Cylindrical Test Specimens and Verifying Conformance to Dimensional and Shape Tolerances*; ASTM D4543-08; ASTM: West Conshohocken, PA, USA, 2008.
22. ISRM. Suggested Methods for Determining the Uniaxial Compressive Strength and Deformability of Rock Materials. *Int. J. Rock Mech. Min. Sci. Geomech. Abstr*. **1979**, *16*, 138–140.
23. ASTM International. *Standard Test Method for Elastic Moduli of Intact Rock Core Specimens in Uniaxial Compression*; ASTM D3148-02; ASTM: West Conshohocken, PA, USA, 2002.

24. Zhou, Y.X.; Xia, K.; Li, X.B.; Li, H.B.; Ma, G.W.; Zhao, J.; Zhou, Z.L.; Dai, F. Suggested Methods for Determining the Dynamic Strength Parameters and Mode-I Fracture Toughness of Rock Materials. *Int. J. Rock Mech. Min. Sci.* **2012**, *49*, 105–112.